Article

Evaluation of the In Vitro and In Vivo Antitumor Efficacy of Peanut Sprout Extracts Cultivated with Fermented Sawdust Medium Against Bladder Cancer

Hongbeom Park [1] , Jun-Hui Song [1] , Byungdoo Hwang [1], BoKyung Moon [1], Seok-Joong Yun [2], Wun-Jae Kim [2,3] and Sung-Kwon Moon [1,*]

[1] Department of Food and Nutrition, Chung-Ang University, Anseong 17546, Korea; hbpencil59@cau.ac.kr (H.P.); goodabc123@cau.ac.kr (J.-H.S.); byungdoo0409@naver.com (B.H.); bkmoon@cau.ac.kr (B.M.)

[2] Department of Urology, Chungbuk National University, Cheongju 361-763, Chungbuk, Korea; sjyun@chungbuk.ac.kr (S.-J.Y.); wjkim@chungbuk.ac.kr (W.-J.K.)

[3] Institute of Urotech, Cheongju 361-763, Chungbuk, Korea

* Correspondence: sumoon66@cau.ac.kr; Tel.: +82-31-670-3284; Fax: +82-31-675-4853

check for updates

Featured Application: This study reveals the anti-tumor action of PSEFS against bladder cancer and suggests its potential to be a promising effective nutraceutical for the treatment of bladder cancer.

Abstract: Peanut sprout extracts reportedly exhibit numerous beneficial effects; however, there are few investigations on the biological effects of peanut sprout extracts cultivated with fermented sawdust medium (PSEFS). Here, we examined whether PSEFS demonstrates antitumor activity against bladder cancer, in vitro and in vivo. The results showed that PSEFS prohibited the proliferation of bladder cancer T24 cells, with this effect attributed to induction of cell cycle arrest at the G1 phase through reduced expression of cyclins and cyclin-dependent kinases caused by a promotion of p21^{WAF1} expression. Additionally, PSEFS induced phosphorylation of p38 mitogen-activated protein kinase. Moreover, PSEFS treatment attenuated the invasive and migratory potential of T24 cells due to decreased matrix metalloproteinase-9 activity combined with downregulation of the transcriptional binding activity of SP1, activator protein -1, and nuclear factor-kappaB. Furthermore, PSEFS (20 mg/kg) attenuated the tumor-growth rate in xenograft mice bearing T24 cells, with an effect equivalent to that of cisplatin and in the absence of toxicity following weight-loss evaluation and hematobiochemical testing of PSEFS-treated mice. These results demonstrated the antitumor efficacy of PSEFS both in vitro and in vivo, thereby reporting it as a potential candidate for development of novel agents against bladder cancer.

Keywords: peanut sprout extracts; fermented sawdust medium; bladder cancer; cell cycle; p38 MAPK; migration; xenograft mice

1. Introduction

Bladder tumors are among the most fatal urological cancers worldwide, with 2 million recorded deaths in 2018 [1]. Most bladder tumors are composed of transitional cell carcinomas comprising non-muscle-invasive bladder cancer (NMIBC) or muscle-invasive bladder cancer (MIBC) [2]. The major approaches to treating NMIBC are straightforward transurethral resection and chemotherapy; however, chemotherapy, hormone therapy, radiotherapy, and surgery are used to treat MIBC, although their therapeutic effect and safety remain undetermined, and MIBC frequently results

in high metastasis, poor prognosis, and death [3–5]. Thus, it is important to develop effective therapeutic agents with minimal adverse reactions to treat bladder cancer.

The abnormal progression of bladder cancer cells emerging from urothelial tumor tissues is linked to multiple cascade signaling pathways involving phosphorylated signaling molecules, including phosphoinositide 3-kinase/AKT (AKT) and mitogen-activated protein kinases (MAPKs), which include extracellular-signal-regulated kinase (ERK)1/2, p38 mitogen-activated protein kinase (p38 MAPK), and c-Jun N-terminal kinase (JNK) [6–8]. Dysregulation of tumor cell proliferation results from a progression of the cell cycle at the G1, S, and G2/M phases, with transition from G1 to S phase controlled by cell cycle regulators [9,10]. These regulators include cyclins, cyclin-dependent kinases (CDKs), and p21^{WAF1}, which have recently received attention as primary targets for antitumor molecules [11,12]. Additionally, tumor-associated matrix metalloproteinases (MMPs) that promote the migratory potential and invasiveness of tumor cells are another attractive target [13,14]. MMP-9 activity reportedly induces invasive and migratory potential that correlated with the progression and occurrence of bladder cancer [6,14,15]. Moreover, during bladder-tumor-derived invasion and migration, MMP-9-related regulatory mechanisms are closely involved in the binding ability of the transcription factors SP1, nuclear factor-kappaB (NF-κB), and activator protein (AP)-1 [16–18].

Resveratrol is a well-known polyphenol compound obtained from grape and peanut sprouts [19,20], and resveratrol-enriched peanut sprout extracts acquired by hydroponic technology have attracted attention for their anti-obesity, anti-oxidative, and anti-inflammatory effects in humans [21–24]. We recently reported that peanut sprout extracts cultivated with fermented sawdust medium (PSEFS) contained higher levels of resveratrol than those obtained with hydroponic technology [25,26]. Additionally, we demonstrated the in vitro and in vivo inhibitory effects of PSEFS in benign prostatic hyperplasia (BPH) [26]. In the present study, we examined for the first time the antitumor efficacy of PSEFS against bladder cancer both in vitro and in vivo. Thus, these results may provide critical information for developing preventive or therapeutic resources for bladder cancer.

2. Materials and Methods

2.1. Materials

Anti-rabbit polyclonal anti-phospho-AKT (9271S), anti-phospho-ERK (9101S), anti-phospho-JNK (9251S), anti-phospho-p38 MAPK (9211S), anti-AKT (9272S), anti-ERK (9102S), anti-JNK (9258S), anti-p38 MAPK (9212S), and anti-p21WAF1 (2947S) antibodies were obtained from Cell Signaling Technology (Danvers, MA, USA). Anti-rabbit polyclonal antibodies against MMP-9 (2395645) were obtained from Millipore Sigma (Burlington, MA, USA). Anti-mouse polyclonal antibodies against CDK2 (sc-163), CDK4 (sc-23896), cyclin D1 (sc-8396), cyclin E (sc-247), p27^{KIP1} (sc-1641), p53 (sc-126), glyceraldehyde 3-phosphate dehydrogenase (GAPDH; sc-47724), HSP70 (sc-24), and SB203580 (sc-3533) were purchased from Santa Cruz Biotechnology (Dallas, TX, USA).

2.2. Sample Preparation

PSEFS was prepared as reported previously [26]. Briefly, to prepare the sawdust medium, oak sawdust and peanut hull mixture were combined at a ratio of 9:1 (*w/w*), and moisture content and temperature were adjusted to 50% and 20 °C, respectively, for 45 days of fermentation. Korean peanut varieties were sprouted for 9 days by utilizing a fermented sawdust medium, and samples were lyophilized (FreeZone; Labconco, Kansas City, MO, USA) at −80 °C and 0.08 Mbar, pulverized (HMF-3000S; Gwanju, Korea), and stored at −70 °C for further analysis. PSEFS was prepared using the Yesan variety containing the highest concentration of resveratrol [26]. To perform extraction, ethanol and water were added to the dried peanut sprouts. After concentration of the extracts, they were dried and stored for further experiments.

2.3. Cell Culture

The human bladder cancer T24 cell line and BdFC normal bladder cell line were obtained from American Type Culture Collection (ATCC, Manassas, VA, USA) and cultured in Dulbecco's modified Eagle medium (Corning, Corning, NY, USA) containing L-glutamine, 4.5 g/L glucose and sodium pyruvate and supplemented with 50 mL fetal bovine serum (FBS) and 5 mL penicillin (Corning) under a 5% CO_2 humidified incubator at 37 °C.

2.4. PSEFS Treatment, MTT Assay, and Cell Counting

Cells (3×10^4) were seeded and incubated with PSEFS (0, 400, 600, or 800 μg/mL) for 24 h. Dimethyl thiazolyl diphenyl tetrazolium salt (MTT, 5 mL/mL) solution was then mixed with the medium at a 1:10 (*v/v*) ratio, and 100 μL was dispensed into each well at 37 °C. After 4 h, the supernatant was removed, and 200 μL dimethyl sulfoxide was dispensed into each well. Optical density was measured using a 540 nm using an enzyme-linked immunosorbent assay reader (Thermo Fisher Scientific, Rockford, IL, USA). Images of cell morphology were observed using a phase-contrast microscope. For cell counting, cells were detached using 0.25% trypsin supplemented with 0.2% EDTA (Thermo Fisher Scientific), harvested, and gently mixed with 50 μL of 0.4% Trypan Blue (Sigma-Aldrich, St. Louis, MO, USA). Counts of viable cells stained with Trypan Blue were determined using a hemocytometer.

2.5. Cell Cycle Analysis

Cells (5×10^3) were seeded and fixed in pre-cooled 70% ethanol at −20 °C. After 4 h, cell pellets were washed twice with phosphate-buffered saline (PBS) and incubated with DNA-intercalating dye, RNase, and propidium iodide at room temperature for 30 min in the dark. Values for the distribution of the cell cycle were estimated using a Becton-Dickinson flow cytometer (BD Bioscience, Franklin Lakes, NJ, USA) and BD Cellfit software.

2.6. Immunoblots and IP

T24 cells (5×10^6) were incubated with various concentrations of PSESF (0, 400, 600, and 800 μg/mL) at 37 °C for 24 h in a 5% CO_2 humidified incubator. Cells were collected, washed twice with cold PBS, and freeze-thawed in a 150 μL lysis buffer (50 mM HEPES (pH 8.0), 150 mM NaCl, 1 mM EGTA, 1 mM EDTA, 1 mM DTT, 0.1 mM Na_3VO_4, 10 mM β-glycerophosphate, 1 mM NaF, 0.1 mM PMSF, 0.1 mM 10% glycerol, 10 μg/mL leupeptin, 0.1% Tween-20, and 2 μg/mL aprotinin). Cells were harvested and centrifuged at 4 °C for 10 min, and protein concentrations were measured using a BCA reagent kit (Thermo Fisher Scientific). Subsequently, 20 μg of protein was resolved by sodium dodecyl sulfate polyacrylamide gel electrophoresis (SDS-PAGE) using a 10% acrylamide gel, followed by transfer onto nitrocellulose membranes (Hybond; GE Healthcare Life Sciences, Marlborough, MA, USA). Membranes were blocked by incubation with 5% bovine serum albumin (MP Biomedicals, Solon, OH, USA) and reacted with specific primary antibodies at 4 °C for 12 h, after which the membranes were further incubated with corresponding horseradish peroxidase-conjugated secondary antibodies for 2 h at room temperature. A chemiluminescence reagent kit (GE Healthcare Life Sciences) was used to visualize the immunocomplexes. For IP assays, cell lysates were reacted with the corresponding antibodies at 4 °C overnight, and immunocomplexes were captured using protein A-sepharose beads (Santa Cruz Biotechnology) at 4 °C for 2 h. Immunoprecipitated beads were washed and incubated in SDS-PAGE sample buffer supplemented with β-mercaptoethanol (Bio-Rad, Richmond, CA, USA), and immunoprecipitated proteins were loaded and separated using SDS-PAGE, followed by immunoblotting with specific antibodies. All experiments were performed in triplicate. Antibodies against non-phosphorylated forms of signaling proteins and GAPDH were applied as loading controls.

2.7. Apoptosis Assay

Quantification of histone-complexed DNA fragments was employed using Cell Death Detection ELISA Plus Kit (Roche Diagnostics). Briefly, cells were seeded and treated with PSEFS for 24 h in 96 well plates. Then, cells were collected and incubated with lysis buffer. After centrifugation, supernatants were reacted with anti-DNA antibody (peroxidase-conjugated) and anti-histone antibody (biotin-labeled) in a streptavidin-coated 96-well microplate. The absorbance at 405 nm was quantitated via a microplate ELISA reader.

2.8. Wound-Healing Migration Assay

Wound-healing migration assay was performed using modified standard method [27]. T24 cells were added to 3 mL growth medium in 6-well plates and cultured to 90% confluence. To abrogate the migratory potential mediated by cell proliferation, 5 μg/mL mitomycin C (Sigma-Aldrich) was added to each well and incubated for 2 h. Wounds were generated using a sterile 200-μL pipette tip and then treated with PSESF (0, 400, 600, or 800 μg/mL) for 24 h. The wound area was evaluated for cell migration under a microscope (40×; Optica, Ponteranica, Italy).

2.9. Boyden Chamber Invasion Assay

For the invasion assays [28], 24-well inserts (8-μm pore size; SPL Life Sciences, Pocheon-si, Korea) were coated with 0.1% gelatin for 1 h. The cells were incubated with FBS-free media containing mitomycin C (5 μg/mL) for 24 h. Cell resuspensions (3×10^4) were seeded in the upper chamber, to which PSESF (0, 400, 600, and 800 μg/mL) was added, and the bottom chamber contained 500 μL growth medium. The chamber was incubated for 24 h and then washed with PBS. Cells invading through Matrigel at the lower side of the upper chamber were fixed, stained with Crystal Violet, and photographed under an inverted microscope (40×; Optica).

2.10. Zymography

Cells were cultured and incubated with various concentrations of PSEFS for 24 h. Then, the culture supernatants were collected and resolved on a polyacrylamide gel supplemented with 0.25% gelatin. The gel was washed with 2.5% Triton X-100 twice at room temperature. After washing with 15 min, the gel was continuously resuspended in a reaction buffer (50 mM Tris-HCl, 150 mM NaCl, and 10 mM $CaCl_2$; pH 7.5) at 37 °C overnight. The gel staining was performed using 0.2% Coomassie Blue, then followed by de-staining in a solution composing 10% methanol and 10% acetic acid. Clear bands appeared by enzymatic activity on a dark-blue background were photographed on a light box. Gelatinolytic activity of MMP-2 or MMP-9 were evaluated using densitometric quantification.

2.11. Nuclear Extracts and EMSA

EMSA assay was used by modified method [29]. T24 cells were incubated with indicated concentrations of PSEFS (0, 400, 600, and 800 μg/mL) for 24 h. Collected cells were cleaned and resuspended in a buffer composing 10 mM HEPES (pH 8.0), 0.1 mM EDTA, 1 mM DTT, 10 mM KCl, 0.5 mM PMSF, and 0.1 mM EGTA. Cellular pellets were maintained on ice for 15 min and lysed using 0.5% NP-40. Thereafter, nuclear extracts were harvested and extracted utilizing an ice-cold high-salt buffer (20 mM HEPES pH 7.9; 400 mM NaCl; 1 mM each of DTT, PMSF, EDTA and EGTA) at 4 °C for 15 min. Finally, the supernatant including the nuclear extract was obtained by performing centrifugation. The concentrations of proteins were determined via use of BCA protein assay reagent kit (Thermo Fisher Scientific). The nuclear extracts (20 μg) were pre-reacted at 4 °C for 30 min utilizing a 100-fold excess of unlabeled oligonucleotide probes, which is consist of the −79 position of the MMP-9 cis-element of interest. Sequences of oligonucleotides were as follows: Sp-1, GCCCATTCCTTCCGCCCCCAGATGAAGCAG; AP-1, CTGACCCCTGAGTCAGCACTT; and NF-κB, CAGTGGAATTCCCCAGCC. The oligonucleotides

corresponding to the DNA-binding motif of the MMP-9 promoters were reacted with Klenow end-labeled [γ–P ^{32}] ATP utilizing T$_4$–polynucleotide kinase (50,000 cpm/ng). Nuclear extracts were incubated with 2 μg poly dI/dC and ^{32}P-labeled DNA probe in a buffer (25 mM HEPES pH 7.9; 0.5 mM each of EDTA and DTT; 50 mM NaCl; 2.5% glycerol) at 4 °C for 20 min. Finally, the DNA-protein complex was separated by electrophoresis using a 6% polyacrylamide gel at 4 °C, and then, the gel was imaged by exposing the X-ray film. The value of the blots was estimated using ImagePro Plus 6.0 software (Media Cybernetics, Rockville, MD, USA).

2.12. Mouse Xenograft Inoculation

The animal experiments were approved by the Institutional Animal Care and Use Committee of Chung-Ang University. All animal studies were randomly performed. For tumor formation of xenografts, approximately bladder cancer T24 cells (1×10^7 cells/mouse) were injected subcutaneously into the 6-week-old male Balb/C nude mice (n = 5 per group). All mice were exposed to indicated concentrations of PSEFS (0, 20, and 200 mg/kg) by gavage daily. Antitumor efficacy was estimated by comparing with 5 mg/kg cisplatin treatment used as a positive control. The tumor volume and body weight of each mouse were evaluated every 2–3 days. After treatment, mice were sacrificed, and weight and volume of tumor mass were measured.

2.13. Immunohistochemistry

Tumor tissues from xenograft mice were obtained, fixed in 10% formalin solution (Sigma-Aldrich, MO, USA). Tissues were then dehydrated using ethanol, embedded in paraffin, and sectioned. Sequentially, the paraffin-embedded slide was stained with H&E and Ki-67. The tissue slides were observed using a fluorescence microscope.

2.14. Plasma Preparation and Biochemical Analysis

Blood samples were harvested and stored at room temperature for 2 h, and sera were obtained by using centrifuge at $3000\times g$ for 40 min at 4 °C. Sera were analyzed for biochemical parameters in plasma, including alanine aminotransferase (ALT), aspartate aminotransferase (AST), and creatine kinase (CK), using analytical detection kits (Abcam, Burlingame, CA, USA).

2.15. Statistical Analysis

Where appropriate, data obtained from triplicate experiments were expressed as the mean ± the standard deviation (SD). Differences between groups were analyzed using a factorial analysis of variance and Fisher's least significant difference test. A $p < 0.05$ was considered statistically significant.

3. Results

3.1. PSEFS Prohibits the Proliferation of Bladder Cancer T24 Cells by Stimulating Cell Cycle Arrest at the G1 Phase

To investigate the inhibitory effect of PSEFS on the proliferation of bladder cancer T 24 cells, we employed both cell-counting and MTT assays. Trypan Blue staining showed that treatment of T24 cells with PSEFS revealed concentration- and time-dependent decrease in the number of viable cells compared to that of the control (Figure 1B and Figure S1B), with the results of MTT assays supporting these results (Figure 1A and Figure S1A). In addition, up to 800 μg/mL, PSEFS treatment had no effect on growth inhibition of BdFC normal bladder cells (Figure S2A,B). In proliferation assays, we determined an IC$_{50}$ of 800 μg/mL in T24 cells and observed both decreased cell number and diminished cell density according to phase-contrast microscopy (Figure 1C). Moreover, generation of fluorescence-activated cell sorting (FACS) histograms to determine whether PSEFS-induced anti-proliferative effects in T24 cells were related to changes in cell cycle progression indicated that PSEFS treatment induced G1-phase arrest (Figure 1D–H). To investigate the cell death level in PSEFS-treated T24 cells, ELISA-based

apoptosis assay was performed. PSEFS treatment did not affect cell death in T24 cells (Figure S4A). These results indicated that PSEFS treatment enhanced the proliferative inhibition of bladder cancer T24 cells by inducing cell cycle arrest at the G1 phase.
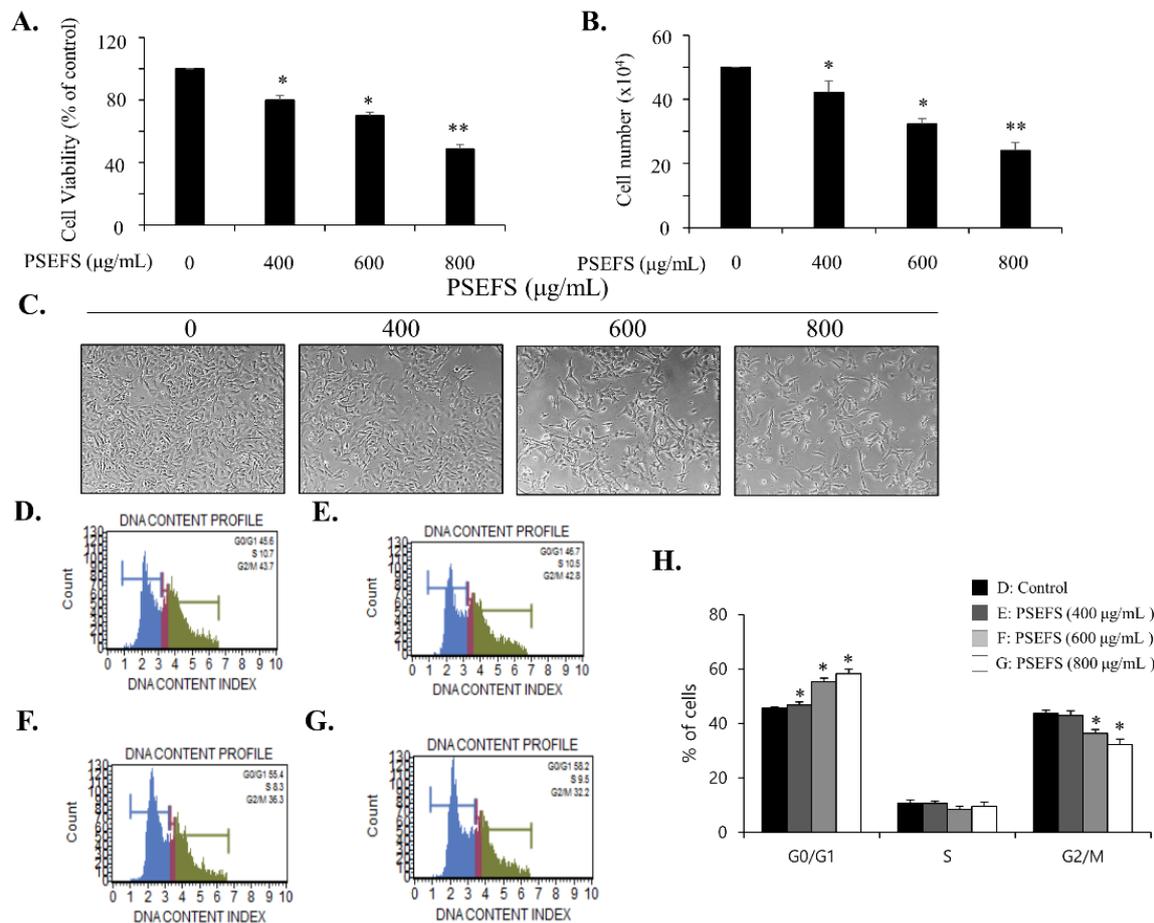
Figure 1. Peanut sprout extracts cultivated with fermented sawdust medium (PSEFS) inhibits T24 cell proliferation via G1-phase arrest. (**A**) Cells were exposed to different concentrations of PSEFS (0, 400, 600, and 800 µg/mL) for 24 h, and an MTT assay was performed to evaluate cell viability. (**B**) Cell counting was performed to determine cell growth. (**C**) Morphological changes of cells according to phase-contrast microscopy (40×). (**D–G**) The cell cycle distribution of T24 cells treated with the indicated concentrations of PSEFS for 24 h and evaluated by flow cytometry analysis. (**H**) The percentage of the cell population in specific cell cycle phases. Data represent the mean ± SD of triplicate experiments. * $p < 0.05$, ** $p < 0.01$ vs. control.

3.2. PSEFS Stimulates G1-Phase Arrest of the Cell Cycle Via Reduced Expression of CDKs and Cyclins by Increasing p21^{WAF1} Protein Level

To determine the precise mechanism associated with cell cycle arrest at the G1 phase in PSEFS-treated T24 cells, we evaluated the levels of cell cycle-related proteins positively modulating the transition from G1 to S phase. The results showed that PSEFS treatment reduced the expression level of CDK4 and its counterpart cyclin D1 in T24 cells (Figure 2A). Additionally, levels of both CDK2 and cyclin E decreased in the presence of PSEFS (Figure 2A). We then examined levels of p21^{WAF1} and p27^{KIP1} as negative regulators of the cell cycle in PSEFS-treated cells. We found that PSEFS treatment upregulated p21^{WAF1} levels with no effect on p27^{KIP1} levels or levels of the tumor suppressor p53 (Figure 2B). Because p21^{WAF1} is reportedly a critical regulator of cell cycle transition from G1 to S phase, we performed immunoprecipitation (IP) experiments using the anti-CDK2 and anti-CDK4

antibodies and detected immunocomplex formation by immunoblot using an anti-p21^{WAF1} antibody. IP experiments indicated that PSEFS treatment markedly upregulated p21^{WAF1} levels according to the observed complex formation with both CDK4 and CDK2 in T24 cells (Figure 2C). These results suggested that PSEFS elicited G1-phase cell cycle arrest through suppression of cyclin and CDK expression via upregulated p21^{WAF1} levels.
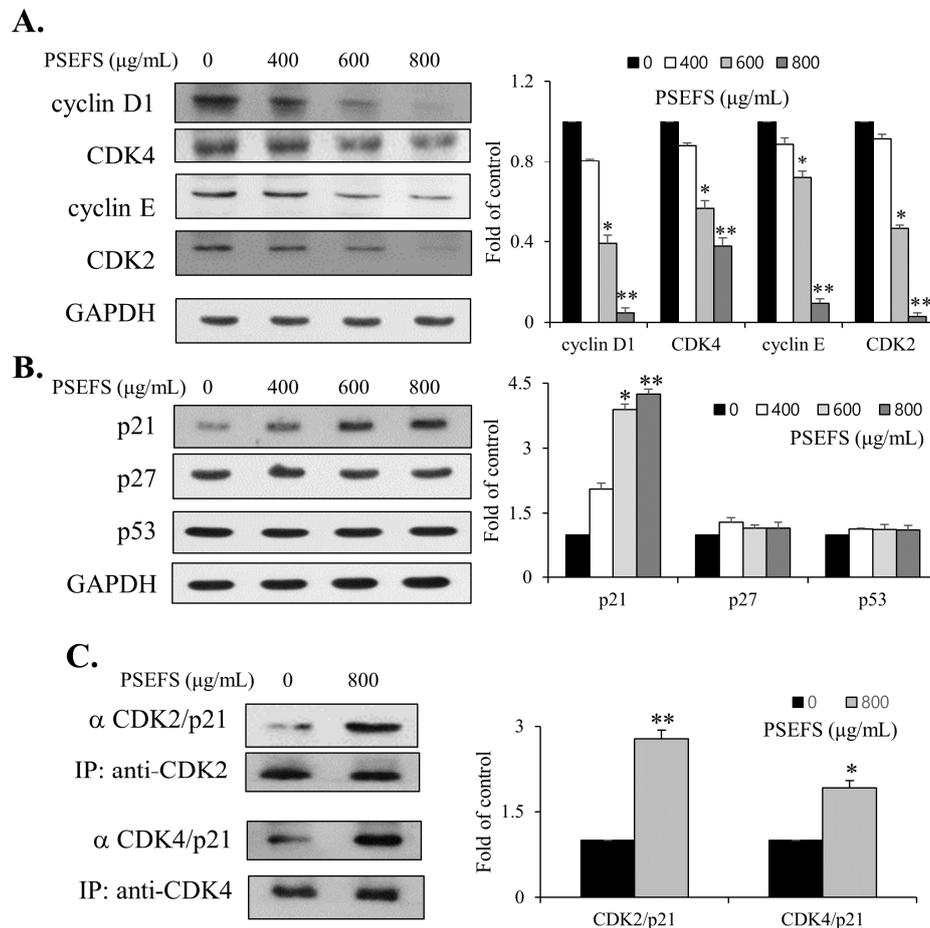
Figure 2. Involvement of cell cycle regulators in PSEFS-mediated cell cycle arrest at the G1 phase. (**A**,**B**) Immunoblot images of CDK4, cyclin D1, CDK2, cyclin E, p21^{WAF1}, p53, and p27^{KIP1} after treatment of T24 cells with PSEFS for 24 h. GAPDH was used as an internal control. (**C**) Cell lysates were immunoprecipitated with anti-CDK4 and anti-CDK2 antibodies, followed by immunoblot with the anti-p21^{WAF1} antibody. Data represent the mean ± SD of triplicate experiments. * $p < 0.05$, ** $p < 0.01$ vs. control.

3.3. PSEFS Suppresses the Phosphorylation of p38 MAPK in T24 Cells

Several studies demonstrated that cytoplasmic early signaling molecules, such as MAPKs (p38 MAPK, JNK, and ERK) and AKT, play crucial roles in mediating the progression and development of bladder tumors [6–8]. Therefore, we investigated whether the phosphorylation levels of AKT and MAPKs are affected by PSEFS in T24 cells. PSEFS treatment induced phosphorylation of p38 MAPK in T24 cells, whereas levels of phosphorylated ERK, JNK, and AKT remained unchanged (Figure 3A–D). To further analyze the direct action of PSEFS on p38 MAPK phosphorylation, we employed the p38 MAPK inhibitor SB203580, finding that SB203580 treatment effectively attenuated phosphorylation of p38 MAPK in PSEFS-treated T24 cells (Figure 3E). In addition, SB203580 treatment reversed PSEFS effect on T24 cell proliferation (Figure S3A,B). These results suggested that PSEFS might stimulate the growth inhibition of T24 cells by inducing p38 MAPK phosphorylation.
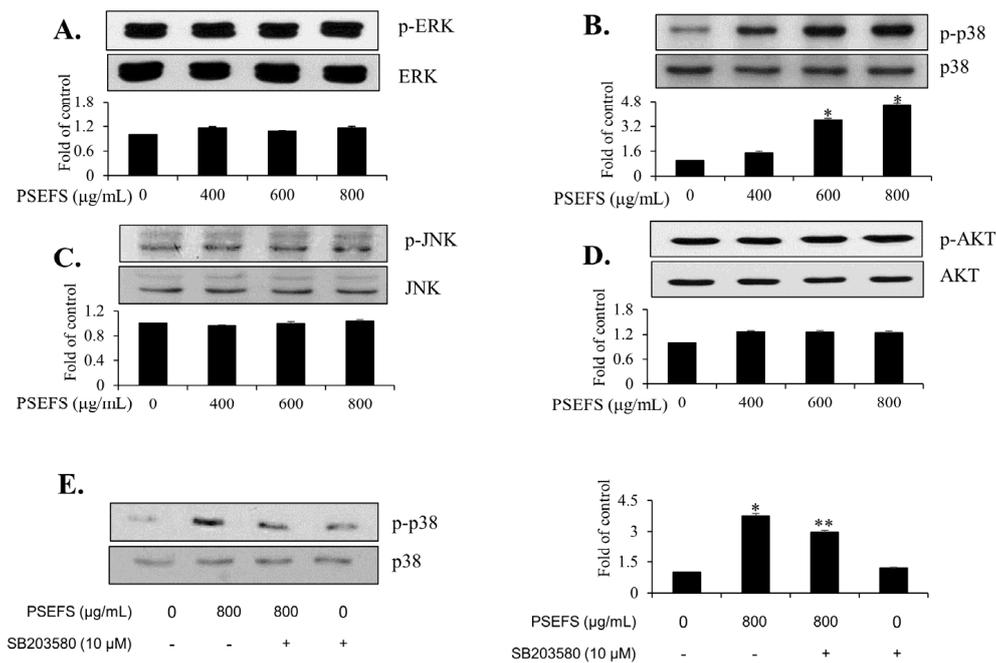
Figure 3. PSEFS promotes the phosphorylation of p38 MAPK in T24 cells. (**A–D**) Changes in phosphorylated levels of MAPKs (JNK, ERK1/2, and p38 MAPK) and AKT according to immunoblot. (**E**) Verification of p38 MAPK phosphorylation using SB203580 (a specific p38 MAPK inhibitor). Bar graphs show fold-changes in expression relative to controls. Data represent the mean ± SD of triplicate experiments. * $p < 0.05$, PSEFS-treated group vs. control; ** $p < 0.05$, PSEFS+SB203580-treated group vs. PSEFS-treated group.

3.4. The MMP-9-Related Transcription Factors SP1, AP-1, and NF-κB are Associated with PSEFS-Induced Mitigation of T24 Cell Migration and Invasion

To determine the migration and invasion capability of PSEFS-treated T24 cells, we performed both wound-healing and invasion assays. We evaluated migration potential using a wound-healing assay by shifting the cells into the wound region. Wound closure by T24 cells was hindered by addition of PSEFS (Figure 4A). Additionally, we estimated the invasive ability of T24 cells according to their potential to invade transwell plates using a Boyden chamber assay. Compared with untreated cells, we found that PSEFS treatment prevented cells from crossing the transwell basement membrane (Figure 4B). A recent study reported that the activity of MMPs, including MMP-9 and MMP-2, decomposes the extracellular matrix, thereby promoting the invasiveness and migratory ability of bladder cancer cells [13–15]. Therefore, we performed a gelatin zymography assay to clarify the enzymatic activities of MMP-9 and MMP-2 in PSEFS-treated T24 cells. As shown in Figure 4C, PSEFS treatment blocked MMP-9 activity in T24 cells, although MMP-2 activity remained unchanged, and we observed attenuated levels of MMP-9 protein. Many studies have shown that MMPs were regulated by heat shock proteins [30–32]. Therefore, we investigated whether PSEFS suppresses the expression level of HSP70 in T24 cells. Immunoblot analysis revealed that PSEFS treatment did not affect the HSP70 level in T24 cells (Figure S4B). Finally, to determine the regulatory mechanism of PSEFS-mediated inhibition of MMP-9 activity/expression, we performed an electrophoretic mobility shift assay (EMSA) using oligonucleotides comprising common sequences targeted by SP1, AP-1, and NF-κB. The EMSA results indicated that PSEFS disrupted the binding of each transcription factor to the cis-element of MMP-9 in T24 cells (Figure 4D). These data indicated that PSEFS might impede the migratory potential and invasive ability of T24 cells in part by reducing MMP-9 activity mediated by transcription factors.
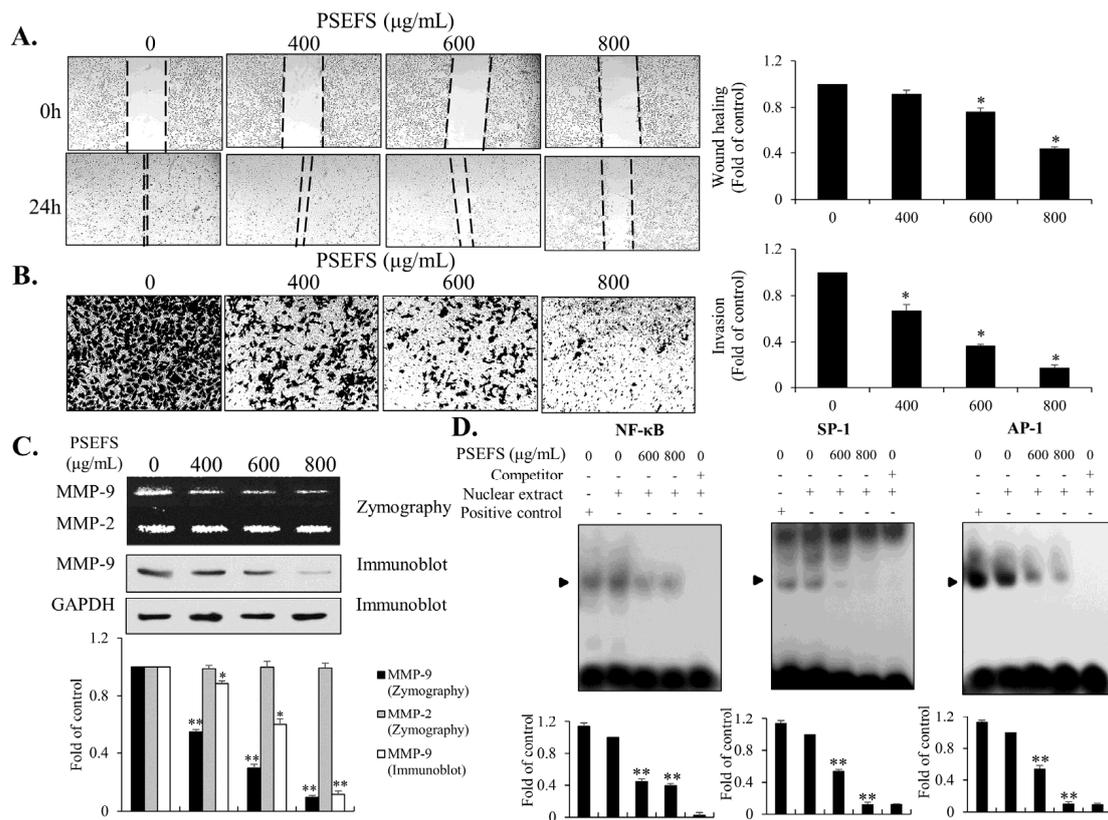
Figure 4. PSEFS inhibits T24 cell migration and invasion by reducing MMP-9 activity and expression through transcriptional repression. T24 cells were incubated with the indicated concentrations of PSEFS for 24 h. (**A**) Migratory potential was investigated (40× magnification) by a wound-healing migration assay. (**B**) T24 cell invasiveness was estimated using a Matrigel-coated chamber transwell assay. (**C**) Both MMP-2 and MMP-9 activity were assessed by gelatin zymography. Relative protein levels of MMP-9 were examined by immunoblot. (**D**) Investigation of DNA binding by SP1, NF-κB, and AP-1 to the cis-element of the MMP-9 promoter according to EMSA. Data represent the mean ± SD of triplicate experiments. * $p < 0.05$, ** $p < 0.01$ vs. control.

3.5. PSEFS Abolishes Tumor Growth in Xenograft Model Bearing Bladder Cancer T24 Cells

To estimate the antitumor efficacy of PSEFS in vivo, various concentrations of PSEFS (0. 20, and 200 mg/kg) were administered by oral gavage to nude mice harboring T24 tumor xenografts, with the chemotherapy drug cisplatin (5 mg/kg) used to compare side effects and antitumor efficacy. Administration of PSEFS promoted a dose-dependent decrease in tumor growth in xenografted mice (Figure 5A). Additionally, both Ki-67 and hematoxylin and eosin (H&E) staining of tumor tissues revealed a diminished number of tumor cells in PSEFS-treated mice (Figure 5D), and tumor volume in PSEFS-treated mice was also reduced relative to controls (Figure 5B). Measurement of weight loss to assess the potential side effects of PSEFS treatment revealed that body weight remained unchanged in PSEFS-treated nude mice, whereas those administered cisplatin showed a ~20% decline in body weight (Figure 5C). Moreover, plasma activities of the liver enzymes alanine transaminase (ALT) and aspartate transaminase (AST) were similar between PSEFS-treated mice and controls (Figure 5E), and no clear difference was observed in the activity of the heart-specific enzyme creatine kinase (CK) between PSEFS-treated and control mice (Figure 5E). These results supported the hypothesis that PSEFS does not produce negative side effects.
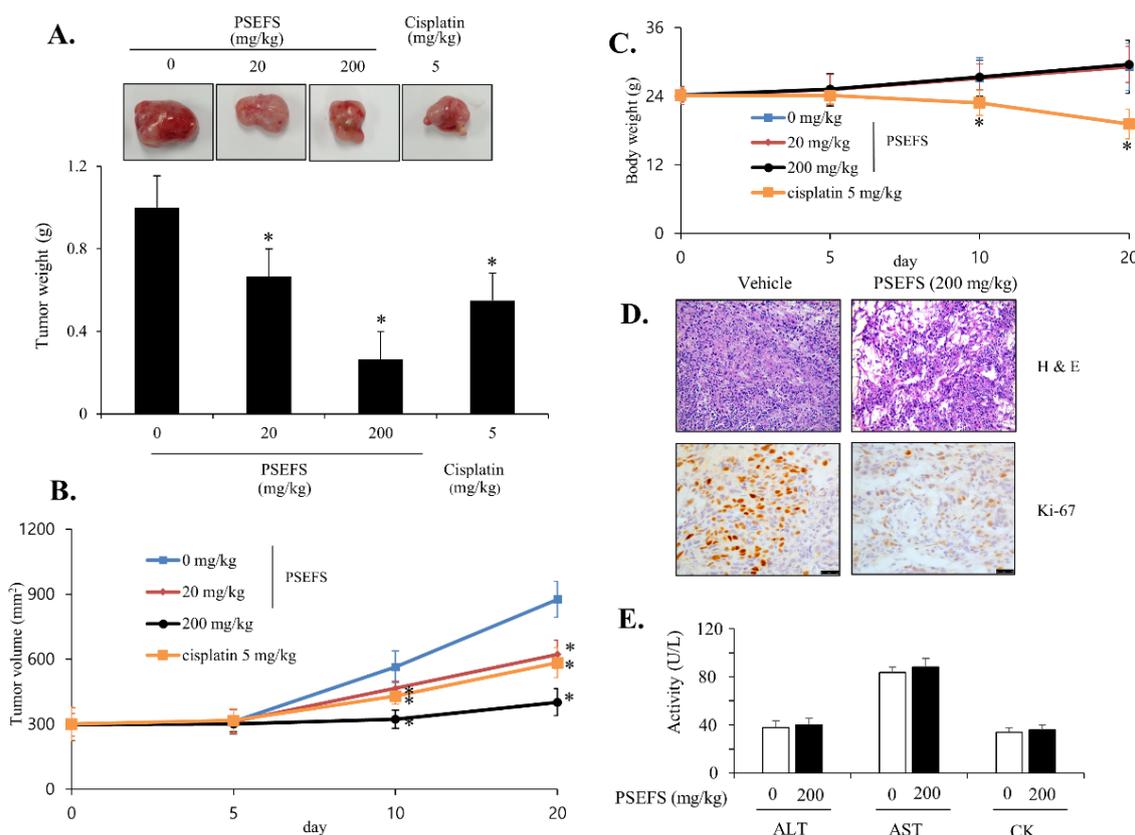
Figure 5. Antitumor efficacy of PSEFS in xenografted mice transplanted with T24 cells. The indicated concentrations of PSEFS (0. 20, and 200 mg/kg) and cisplatin (5 mg/kg; positive control) were orally administered to compare antitumor efficacy. (**A**) Appearance and quantification of weights of tumors separated from xenografted mice following treatment with PSEFS or cisplatin. (**B**) Tumor volumes were evaluated daily in xenografted mice. (**C**) Body weight loss was assessed during PSEFS administration and cisplatin treatment. (**D**) H&E and Ki-67 staining were performed to evaluate tumor growth. (**E**) After treatment with PSEFS, hematobiochemical markers (AST, ALT, and CK) were assessed in plasma from xenografted mice. Data represent the mean ± SD (n = 5). * $p < 0.05$ vs. control.

4. Discussion

Multiple reports have demonstrated that peanut sprouts contain high protein content, unsaturated fatty acid content, polyphenolic content, fiber content, and bioactive components [24–26]. Previous studies indicate that high levels of polyphenolic compounds, such as caffeic acid, coumaric acid, hesperidin, trans-arachidin-1, arahypin 2, arahypin 3, resveratrol, IPP, IPD, trans-arachidin-1, trans-arachidin-2 and trans-arachidin-3, are present in peanut sprouts [24–26]. Resverartrol and other phenolic compounds, such as coumaric acid, hesperidin and their respective stilbene derivatives, were induced during seed germination [24,25]. We recently found that PSEFS generate high levels of resveratrol as compared with those cultivated with hydroponic technology [25,26]. In the present study, we investigated the in vitro and in vivo antitumor effects of PSEFS in bladder cancer.

The results demonstrated that PSEFS inhibited the proliferation of bladder cancer T24 cells without cell toxicity. Antitumor agents that mainly function by inhibiting cell cycle transition have previously been developed, as controlling cell cycle regulators responsible for cell cycle progression at specific stages represent promising candidates for the development of antitumor molecules [11,12,33,34]. Previous studies demonstrated that several compounds exerted multiple actions in regulation of cell cycle in cancer cell lines [35–37]. In the present study, we investigated whether PSEFS affects cell cycle progression, with the results indicating that PSEFS treatment induced G1-phase arrest due to

upregulation of the cell cycle inhibitor p21WAF1 and downregulation of CDKs and cyclins in T24 cells. These findings demonstrated that PSEFS inhibited T24 cell proliferation by suppressing cyclin and CDK levels through induction of p21WAF1 expression. This suggests that regulators associated with cell cycle progression might represent molecular targets for PSEFS-mediated clinical applications against bladder cancer.

Previous studies demonstrated the important function of early signaling molecules in various cellular events attributed to cell proliferation and cell cycle progression [7,8,38]. Cumulative reports indicated that some compounds govern cell proliferation through regulation of MAPKs signaling pathway [39,40]. However, information on the antitumor effect of PSEFS relevant to signaling pathways has not been reported. Therefore, we investigated the regulatory mechanism associated with PSEFS-mediated inhibition of T24 cell proliferation and the related signaling pathways involving including AKT and MAPKs (p38 MAPK, JNK, and ERK1/2). The results revealed that PSEFS treatment induced phosphorylation of p38 MAPK. SB203580 treatment attenuated PSEFS-induced inhibition of T24 cell proliferation, suggesting p38 MAPK as a factor partially mediated by suppression of T24 cell proliferation.

Additionally, we demonstrated that PSEFS treatment suppressed T24 cell invasion and migration associated with downregulation of MMP-9 activity in the presence of PSEFS. Several reports indicate MMP-9 activity as essential for the migratory and invasive potential of bladder cancer cells, as MMP-9 induces degradation of the extracellular matrix and promotes progression of tumor cell invasion and migration [6,14,15]. In the present study, we showed that PSEFS repressed T24 cell invasion and migration by reducing MMP-9 activity and expression, specifically through control of AP-1, NF-κB, and SP1 targeting of its promoter region [16–18]. Further investigation of the DNA-binding activity of these transcription factors confirmed that PSEFS treatment decreased their DNA-binding abilities to the MMP-9 promoter region in T24 cells, revealing that PSEFS-mediated suppression of T24 cell invasion and migration is associated with reduced MMP-9 expression and activity as a consequence of decreased transcriptional activation by SP1, NF-κB, and AP-1.

We then evaluated the antitumor efficacy of PSEFS in vivo using a mouse xenograft model. PSEFS administration reduced both tumor volume and weight in xenografted mice bearing bladder T24 tumors, with decreased tumor cell proliferation confirmed by H&E and Ki-7 staining, and establishment of an effective PSEFS dose at 200 mg/kg. Importantly, we identified the antitumor efficacy of 20 mg/kg PSEFS as equivalent value to that of 5 mg/kg cisplatin, although without the observed side effects (i.e., significant loss of body weight or hematobiochemical activity (AST, ALT, and CK)) observed following cisplatin treatment, thereby underscoring the lack of PSEFS-related toxicity. These findings indicated that resveratrol-enriched PSEFS can be utilized for the treatment and prevention of bladder cancer with minimal side effects or natural supplements, although additional studies incorporating detailed toxicity tests for antitumor agents need to be performed.

Our study demonstrates the antitumor efficacy of PSEFS against bladder cancer. PSEFS-induced inhibition of bladder cancer T24 cell proliferation mainly involved in the promotion of G1-phase cell cycle arrest through downregulation of CDKs and cyclins was caused by an increased expression of p21WAF1. Additionally, p38 MAPK phosphorylation increased with PSEFS treatment. The PSEFS-mediated suppressive effect of migration and invasion potential in T24 cells was due to a decreased binding of transcription factors associated with MMP-9 regulation. Moreover, administration of PSEFS abolished tumor growth rate in xenograft mice bearing T24 tumor cells without noticeable side effects. These data suggest PSEFS as an effective and promising candidate antitumor molecule against bladder cancer.

References

1. Bray, F.; Ferlay, J.; Soerjomataram, I.; Siegel, R.L.; Torre, L.A.; Jemal, A. Global Cancer Statistics 2018: GLOBOCAN Estimates of Incidence and Mortality Worldwide for 36 Cancers in 185 Countries. *CA Cancer J. Clin.* **2018**, *68*, 394–424. [CrossRef] [PubMed]

2. Matulay, J.T.; Kamat, A.M. Advances in Risk Stratification of Bladder Cancer to Guide Personalized Medicine. *F1000Research* **2018**, *7*, 1137. [CrossRef] [PubMed]

3. Chromecki, T.F.; Bensalah, K.; Remzi, M.; Verhoest, G.; Cha, E.K.; Scherr, D.S.; Novara, G.; Karakiewicz, P.I.; Shariat, S.F. Prognostic Factors for Upper Urinary Tract Urothelial Carcinoma. *Nat. Rev. Urol.* **2011**, *8*, 440–447. [CrossRef] [PubMed]

4. Berdik, C. Unlocking Bladder Cancer. *Nature* **2017**, *551*, S34–S35. [CrossRef] [PubMed]

5. Ghagane, S.C.; Puranik, S.I.; Kumbar, V.M.; Nerli, R.B.; Jalalpure, S.S.; Hiremath, M.B.; Neelagund, S.; Aladakatti, R. In Vitro Antioxidant and Anticancer Activity of Leea Indica Leaf Extracts on Human Prostate Cancer Cell Lines. *Integr. Med. Res.* **2017**, *6*, 79–87. [CrossRef] [PubMed]

6. Knowles, M.A.; Hurst, C.D. Molecular Biology of Bladder Cancer: New Insights into Pathogenesis and Clinical Diversity. *Nat. Rev. Cancer* **2015**, *15*, 25–41. [CrossRef] [PubMed]

7. Gerhardt, D.; Bertola, G.; Dietrich, F.; Figueiró, F.; Zanotto-Filho, A.; Moreira Fonseca, J.C.; Morrone, F.B.; Barrios, C.H.; Battastini, A.M.O.; Salbego, C.G. Boldine Induces Cell Cycle Arrest and Apoptosis in T24 Human Bladder Cancer Cell Line Via Regulation of ERK, AKT, and GSK-3β. *Urol. Oncol.* **2014**, *32*, 36.e1–36.e9. [CrossRef] [PubMed]

8. Mayer, I.A.; Arteaga, C.L. The PI3K/AKT Pathway as a Target for Cancer Treatment. *Annu. Rev. Med.* **2016**, *67*, 11–28. [CrossRef]

9. Sclafani, R.A.; Holzen, T.M. Cell Cycle Regulation of DNA Replication. *Annu. Rev. Genet* **2007**, *41*, 237–280. [CrossRef]

10. Li, A.; Blow, J.J. The Origin of CDK Regulation. *Nat. Cell Biol.* **2001**, *3*, 182. [CrossRef]

11. Otto, T.; Sicinski, P. Cell Cycle Proteins as Promising Targets in Cancer Therapy. *Nat. Rev. Cancer* **2017**, *17*, 93–115. [CrossRef] [PubMed]

12. Jeggo, P.A.; Pearl, L.H.; Carr, A.M. DNA Repair, Genome Stability and Cancer: A Historical Perspective. *Nat. Rev. Cancer* **2016**, *16*, 35–42. [CrossRef]

13. Robertson, A.G.; Kim, J.; Al-Ahmadie, H.; Bellmunt, J.; Guo, G.; Cherniack, A.D.; Hinoue, T.; Laird, P.W.; Hoadley, K.A.; Akbani, R.; et al. Comprehensive Molecular Characterization of Muscle-Invasive Bladder Cancer. *Cell* **2017**, *171*, 540–556.e25. [CrossRef] [PubMed]

14. Bianco, F.J.; Gervasi, D.C.; Tiguert, R.; Grignon, D.J.; Pontes, J.E.; Crissman, J.D.; Fridman, R.; Wood, D.P. Matrix Metalloproteinase-9 Expression in Bladder Washes from Bladder Cancer Patients Predicts Pathological Stage and Grade. *Clin. Cancer Res.* **1998**, *4*, 3011–3016. [PubMed]

15. Davies, B.; Waxman, J.; Wasan, H.; Abel, P.; Williams, G.; Krausz, T.; Neal, D.; Thomas, D.; Hanby, A.; Balkwill, F. Levels of Matrix Metalloproteases in Bladder Cancer Correlate with Tumor Grade and Invasion. *Cancer Res.* **1993**, *53*, 5365–5369. [PubMed]

16. Bond, M.; Fabunmi, R.P.; Baker, A.H.; Newby, A.C. Synergistic Upregulation of Metalloproteinase-9 by Growth Factors and Inflammatory Cytokines: An Absolute Requirement for Transcription Factor NF-Kappa B. *FEBS Lett.* **1998**, *435*, 29–34. [CrossRef]

17. Sato, H.; Seiki, M. Regulatory Mechanism of 92 kDa Type IV Collagenase Gene Expression which is Associated with Invasiveness of Tumor Cells. *Oncogene* **1993**, *8*, 395–405.

18. Lee, S.; Cho, S.; Lee, E.; Kim, S.; Lee, S.; Lim, J.; Choi, Y.H.; Kim, W.; Moon, S. Interleukin-20 Promotes Migration of Bladder Cancer Cells through Extracellular Signal-Regulated Kinase (ERK)-Mediated MMP-9 Protein Expression Leading to Nuclear Factor (NF-κB) Activation by Inducing the Up-Regulation of p21(WAF1) Protein Expression. *J. Biol. Chem.* **2013**, *288*, 5539–5552. [CrossRef]

19. De Vries, K.; Strydom, M.; Steenkamp, V. Journal of Herbal Medicine. *J. Herb. Med.* **2011**, *11*, 71–77. [CrossRef]

20. Howitz, K.T.; Bitterman, K.J.; Cohen, H.Y.; Lamming, D.W.; Lavu, S.; Wood, J.G.; Zipkin, R.E.; Chung, P.; Kisielewski, A.; Zhang, L.; et al. Small Molecule Activators of Sirtuins Extend Saccharomyces Cerevisiae Lifespan. *Nature* **2003**, *425*, 191–196. [CrossRef]

21. Choi, J.; Choi, D.; Lee, J.; Yun, S.; Lee, D.; Eun, J.; Lee, S. Ethanol Extract of Peanut Sprout Induces Nrf2 Activation and Expression of Antioxidant and Detoxifying Enzymes in Human Dermal Fibroblasts: Implication for its Protection Against UVB-Irradiated Oxidative Stress. *Photochem. Photobiol.* **2013**, *89*, 453–460. [CrossRef] [PubMed]

22. Kang, H.; Kim, J.; Kwon, S.; Park, K.; Kang, J.; Seo, K.I. Antioxidative Effects of Peanut Sprout Extracts. *J. Korean Soc. Food Sci. Nutr.* **2010**, *39*, 941–946. [CrossRef]

23. Kang, N.E.; Ha, A.W.; Woo, H.W.; Kim, W.K. Peanut Sprouts Extract (Arachis Hypogaea L.) has Anti-Obesity Effects by Controlling the Protein Expressions of PPARγ and Adiponectin of Adipose Tissue in Rats Fed High-Fat Diet. *Nutr. Res. Pract.* **2014**, *8*, 158–164. [CrossRef] [PubMed]

24. Limmongkon, A.; Nopprang, P.; Chaikeandee, P.; Somboon, T.; Wongshaya, P.; Pilaisangsuree, V. LC-MS/MS Profiles and Interrelationships between the Anti-Inflammatory Activity, Total Phenolic Content and Antioxidant Potential of Kalasin 2 Cultivar Peanut Sprout Crude Extract. *Food Chem.* **2018**, *239*, 569–578. [CrossRef]

25. Li, T.; Luo, L.; Kim, S.; Moon, S.; Moon, B. Trans-Resveratrol Extraction from Peanut Sprouts Cultivated using Fermented Sawdust Medium and its Antioxidant Activity. *J. Food Sci.* **2020**, *85*, 639–646. [CrossRef] [PubMed]

26. Song, J.H.; Hwang, B.; Chung, H.J.; Moon, B.; Kim, J.W.; Ko, K.; Kim, B.W.; Kim, W.R.; Kim, W.J.; Myung, S.C.; et al. Peanut Sprout Extracts Cultivated with Fermented Sawdust Medium Inhibits Benign Prostatic Hyperplasia in Vitro and in Vivo. *World J. Mens Health* **2020**, *38*, 385–396. [CrossRef] [PubMed]

27. Rodriguez, L.G.; Wu, X.; Guan, J. Wound-Healing Assay. *Methods Mol. Biol.* **2005**, *294*, 23–29.

28. Chen, H. Boyden Chamber Assay. *Methods Mol. Biol.* **2005**, *294*, 15–22.

29. Hellman, L.M.; Fried, M.G. Electrophoretic Mobility Shift Assay (EMSA) for Detecting Protein-Nucleic Acid Interactions. *Nat. Protoc.* **2007**, *2*, 1849–1861. [CrossRef]

30. Qi, Z.; Tang, T.; Sheng, L.; Ma, Y.; Liu, Y.; Yan, L.; Qi, S.; Ling, L.; Zhang, Y. Salidroside Inhibits the Proliferation and Migration of Gastric Cancer Cells Via Suppression of Src associated Signaling Pathway Activation and Heat Shock Protein 70 Expression. *Mol. Med. Rep.* **2018**, *18*, 147–156. [CrossRef]

31. Rajesh, Y.; Banerjee, A.; Pal, I.; Biswas, A.; Das, S.; Dey, K.K.; Kapoor, N.; Ghosh, A.K.; Mitra, P.; Mandal, M. Delineation of Crosstalk between HSP27 and MMP-2/MMP-9: A Synergistic Therapeutic Avenue for Glioblastoma Management. *Biochim. Et Biophys. Acta (BBA)-Gen. Subj.* **2019**, *1863*, 1196–1209. [CrossRef] [PubMed]

32. Sulistyowati, E.; Lee, M.Y.; Wu, L.C.; Hsu, J.H.; Dai, Z.K.; Wu, B.N.; Lin, M.C.; Yeh, J.L. Exogenous Heat Shock Cognate Protein 70 Suppresses LPS-Induced Inflammation by Down-Regulating NF-kappaB through MAPK and MMP-2/-9 Pathways in Macrophages. *Molecules* **2018**, *23*, 2124. [CrossRef] [PubMed]

33. Osborne, C.K.; Boldt, D.H.; Clark, G.M.; Trent, J.M. Effects of Tamoxifen on Human Breast Cancer Cell Cycle Kinetics: Accumulation of Cells in Early G1 Phase. *Cancer Res.* **1983**, *43*, 3583–3585.

34. Lin, H.L.; Chang, Y.F.; Liu, T.Y.; Wu, C.W.; Chi, C.W. Submicromolar Paclitaxel Induces Apoptosis in Human Gastric Cancer Cells at Early G1 Phase. *Anticancer. Res.* **1998**, *18*, 3443–3449. [PubMed]

35. Huang, K.; Kuo, C.; Chen, S.; Lin, C.; Lee, Y. Honokiol Inhibits in Vitro and in Vivo Growth of Oral Squamous Cell Carcinoma through Induction of Apoptosis, Cell Cycle Arrest and Autophagy. *J. Cell. Mol. Med.* **2018**, *22*, 1894–1908. [CrossRef] [PubMed]

36. Li, Y.; Cheng, X.; Chen, C.; Huijuan, W.; Zhao, H.; Liu, W.; Xiang, Z.; Wang, Q. Apigenin, a Flavonoid Constituent Derived from P. Villosa, Inhibits Hepatocellular Carcinoma Cell Growth by CyclinD1/CDK4 Regulation Via p38 MAPK-p21 Signaling. *Pathol.-Res. Pract.* **2020**, *216*, 152701. [CrossRef]

37. Dhatwalia, S.K.; Kumar, M.; Dhawan, D.K. Role of EGCG in Containing the Progression of Lung Tumorigenesis–A Multistage Targeting Approach. *Nutr. Cancer* **2018**, *70*, 334–349. [CrossRef]

38. Kamiyama, M.; Naguro, I.; Ichijo, H. In Vivo Gene Manipulation Reveals the Impact of Stress-Responsive MAPK Pathways on Tumor Progression. *Cancer Sci.* **2015**, *106*, 785–796. [CrossRef]

39. Yu, X.; Zhong, J.; Yan, L.; Li, J.; Wang, H.; Wen, Y.; Zhao, Y. Curcumin Exerts Antitumor Effects in Retinoblastoma Cells by Regulating the JNK and p38 MAPK Pathways. *Int. J. Mol. Med.* **2016**, *38*, 861–868. [CrossRef]

40. Huang, G.; Tang, B.; Tang, K.; Dong, X.; Deng, J.; Liao, L.; Liao, Z.; Yang, H.; He, S. Isoquercitrin Inhibits the Progression of Liver Cancer in Vivo and in Vitro Via the MAPK Signalling Pathway. *Oncol. Rep.* **2014**, *31*, 2377–2384. [CrossRef]

Publisher's Note: MDPI stays neutral with regard to jurisdictional claims in published maps and institutional affiliations.